RESEARCH ARTICLE

INTERNATIONAL RESEARCH JOURNAL OF MULTIDISCIPLINARY TECHNOVATION

Asian Research Association

DOI: 10.54392/irjmt26211

Design and Control of Hybrid Fuel Cell Vehicle Powertrains Using Multi-Objective Genetic Algorithms across Diverse Driving Cycles

Bilal Soltani [a,*], Nedjem-Eddine Benchouia [a], Abdelghani Guechi [a]

[a] Department of Mechanical Engineering, Laboratory of Management, Maintenance and Rehabilitation of Facilities and Urban Infrastructure, University of Souk Ahras, Souk Ahras, 41000 – Algeria.

* Corresponding Author Email: b.soltani@univ-soukahras.dz

DOI: https://doi.org/10.54392/irjmt26211

Received: 01-11-2025; Revised: 17-02-2026; Accepted: 01-03-2026; Published: 20-03-2026

Abstract: Attainment of environmentally friendly methods of transportation is largely contingent upon the availability and practicality of hydrogen fuel cell vehicles (FCVs), but FCVs currently have a number of limitations in establishing their widespread user base due to their excessive hydrogen consumption, high system costs, and difficulty in regulating energy utilization based on the behavior of system operators under highly variable dynamic loads associated with typical transportation activity of users. Therefore, understanding the linkage between the fuel cell energy system and supplementary energy storage systems in the hybrid FCV powertrain is an important determinant of total performance, longevity, and fuel economy. This thesis addresses the issue of reducing hydrogen consumption while maintaining the performance of the energy system through the development of an optimal energy management strategy. MATLAB/Simulink has been used to develop a complete hybrid FCV simulation model using an ultracapacitor-based energy storage system coupled with a PEMFC stack for the purpose of this research. The development and implementation of a multi-objective genetic algorithm (MOGA) were carried out in the development of the hybrid FCV simulation model to mitigate operational limitations (i.e., power balance, SoC limits) and simultaneously reduce hydrogen consumption and maximize system efficiency. The MOGA optimization process was performed under a population-based, evolutionary framework employing the convergence of more than one objective with predefined operational constraints. The optimization framework takes into account both important sizing variables, like fuel cell configuration and ultracapacitor operating limits, and control parameters. To analyze the performance of the combined approach, we simulated various standardized driving cycles alongside an actual route in Algeria—Ouenza to Annaba—chosen for its accuracy in mimicking the conditions under which the evaluated vehicles would be driven. Simulation outputs showed that there were Pareto-optimal values from our analysis, allowing a reduction of hydrogen usage by 30% vs. baseline and greater improvements in energy efficiency and SoC trajectory stability when compared to the baseline method across every tested driving scenario. As a result, optimized designs used smaller and cheaper fuel cells, without compromising the performance of the vehicle. What makes this research unique is that we utilized this methodology to combine multiple standardized driving cycles with an actual route while optimizing both energy management and component sizing parameters through an MOGA framework. Therefore, we provide a means for developing replicable, regionally adaptable advanced fuel cell vehicle powertrain design solutions.

Keywords: Fuel Cell Vehicle, Energy Management Strategy, Multi-Objective Genetic Algorithm, Optimization, Hybrid Powertrain Modeling, Driving Cycle.

1. Introduction

An increase in worldwide environmental consciousness and a diminishing supply of fossil fuels have led to a rapid advancement in the use of utilizing clean energy in the transportation arena. Fuel Cell Vehicles, which are more efficient than Conventional Internal Combustion Engines (ICE) and produce fewer greenhouse gases, in addition to having longer distances that can be driven with one tank of hydrogen, will see an increasing presence on our roads in the near future. [1]. These advantages are largely achieved through advanced energy management and energy storage solutions, which play a crucial role in making transportation systems more sustainable [2]. Nevertheless, FCVs still face major challenges related to hydrogen consumption, system cost, and powertrain sizing, all of which must be optimized to enable competitiveness with conventional internal combustion engine (ICE) vehicles [3]. There has been significant

focus on hybridizing fuel cells to further improve their overall performance and energy efficiency by combining them with auxiliary energy storage devices, such as batteries (in addition to ultracapacitor technology), to achieve a broadly used hybrid fuel cell vehicle [4–6]. While all energy storage technologies can be used in conjunction with fuel cells, ultracapacitors have shown particular promise due to their superior power density characteristics, high charge/discharge rates, and extended lifetimes compared to other energy storage options. These characteristics allow effective transient power support and efficient energy recovery during regenerative braking events [7]. In parallel, several studies have investigated control strategies and powertrain architectures for hydrogen and electric vehicles under real or locally representative driving conditions. The work of Tazerart *et al.* [8] focused specifically upon designing a new method for managing torque, or direct torque control (DTC), for hydrogen-fuel-cell-powered vehicles operating under low-speed (e.g., slow city-driving) conditions. Tazerart *et al.* [9] also focused on minimizing energy losses incurred by induction machines that are used in electric vehicle drive trains. As can be seen from these two publications, there is a strong emphasis within this body of research on the significance of employing sophisticated control techniques to optimize the efficiency of the total vehicle system.

The energy management system (EMS), which determines how power is shared between fuel cells and additional source energy when there are changes in the driving conditions, has an outstanding effect on the operation of hybrid fuel cell vehicle systems. There are many different approaches to EMS that have been described in the literature. Rule-based (RB) methods allow for a simple implementation but usually lack any adaptability for very variable and complicated conditions [10]. Fuzzy logic approaches allow more flexibility in the way that they can deal with non-linear behaviors within the system, but often require heuristic tuning through expert knowledge to perform well [4]. Finally, dynamic programming (DP) and other optimization methods are rigorous and can provide a globally optimum solution, but they place an excessive computational burden on real-time vehicle applications, hence rendering them impractical for online vehicle applications [11].

In addition to classical control methods, intelligent and adaptive strategies have also been explored. Nasri and Gasbaoui [12], for instance, employed a neuro-fuzzy controller to improve traction and safety in four-wheel electric vehicles, demonstrating the feasibility of soft computing techniques in real-time control scenarios. To overcome the limitations of single-objective and computationally intensive approaches, evolutionary optimization techniques—particularly genetic algorithms (GA) and multi-objective genetic algorithms (MOGA)—have attracted increasing interest. These methods enable the simultaneous optimization of conflicting objectives, such as minimizing hydrogen consumption, maximizing system efficiency, and maintaining the state of charge (SoC) of energy storage devices within acceptable limits [6], [13, 14]. Despite their advantages, most existing studies validate their proposed strategies using standardized driving cycles, such as NEDC, FTP, or UDDS, which often fail to capture the complexity of real-world driving behavior and road conditions [15].

In addition, few studies focused on the simultaneous optimization of both control strategy and sizing parameters, such as the number of fuel cell stacks and operational limits of ultracapacitors. The impact of geography-specific factors (i.e., road grade, acceleration patterns induced by traffic, and environmental conditions) is also underrepresented in the literature. The limitations on research in this area are particularly applicable to developing regions like North Africa, where infrastructure characteristics and driving conditions are likely to differ markedly from assumptions made using standardized cycles. Djermouni *et al.* [16] highlighted the importance of considering local conditions in energy management studies through their work on PV-powered electric vehicle charging stations in the Algerian context.

Motivated by these gaps, this research develops an optimal energy management strategy for hybrid FCVs based on a multi-objective genetic algorithm, incorporating both standardized and realistic driving conditions. System performance is evaluated using conventional driving cycles as well as a real-world Algerian route between Ouenza and Annaba (OU12–ANN23), which reflects local traffic dynamics and road characteristics not captured by standardized cycles. The proposed approach simultaneously optimizes fuel cell configuration parameters (including the number of stacks, efficiency, and active area), ultracapacitor operating limits, and power-sharing logic. Running MATLAB/Simulink simulations produced Pareto-optimal trade-offs that associated the following outcomes that had been achieved at 30%: hydrogen consumption reduction, increased compactness, reduced cost of the fuel cell, and increased performance on the global vehicle scale across many different operational conditions.

A summary of the primary contributions of the present study is as follows: (1) Development of a comprehensive fuel cell vehicle model, which incorporates ultracapacitors for the purpose of providing transient power support and regenerative braking; (2) Development of a Multi-Objective Genetic Algorithm - based energy management strategy that optimizes both the sizing of components and the control parameters simultaneously; (3) The introduction of an Algerian real-world route for the purpose of evaluating the robustness of energy management systems against the traffic characteristics present within Algeria; (4) Assessment of hydrogen savings, decreased component costs, and

performance equivalent to that of conventional FCVs; and (5) Presentation of a flexible and scalable framework, which can be tailored to suit different regional restrictions and structural limitations.

1.1 Novelty vs. Prior Work

While previous GA/MOGA-based EMS approaches primarily focused on optimizing control parameters under standardized driving cycles, the proposed method extends these efforts by jointly considering energy management and component sizing within a unified optimization framework. As illustrated in Table 1, the validation portion of this study provides a larger vehicle performance evaluation by incorporating validated standard and region-specific real-world driving conditions. The integrated formulation creates an incremental but substantial advancement to existing GA/MOGA-based EMS strategies for FCV.

2. Modeling of the System

Figure 1 illustrates the general architecture of a proton exchange membrane fuel cell (PEMFC) vehicle, which includes a fuel cell stack, an ultracapacitor system, and a power electronic interface. This structure forms the basis for the hybrid energy management strategy developed in this study. The arrangement of components presented in the figure represents the real system we modeled in our simulations and thus is the physical basis for the control and optimization methods we propose.

The PEMFC system generates electricity based on the chemical reaction of oxygen and hydrogen occurring in the fuel cell stack. The ultracapacitor provides additional power when needed. Power converters control voltage and current, and a continuous bus conducts energy to the machine, providing traction to the vehicle.

The figure represents the energy and power flow architecture of a fuel cell vehicle (FCV). It consists of four key sections:

2.1 Power Sources

- Fuel Cell (FC): A fuel cell serves as the main energy source and provides continuous power based on hydrogen.
- Supercapacitor (SC): In turn, a supercapacitor acts as the secondary energy source, allowing for rapid energy of acceleration and quick demand.

2.2 Static Converters

- DC/DC Boost Converters: Boosts the fuel cell up to a certain voltage level for continuous operating conditions.
- DC/DC Buck-Boost Converters: Provides control over supercapacitor energy supply, either providing or storing energy as required.
- DC/AC Inverter: The device used to convert DC power to power synchronous electric motors.

2.3 Synchronous Electric Motor

Converts electrical energy from the inverter into mechanical energy to propel the vehicle.

2.4 Control Block

- Management of Energy Flow: Regulates the current from the fuel cell and supercapacitor according to power requirements.
- Regulation of Current & Voltage: Maintains power stability.
- Energy Optimization: Maximizes fuel efficiency in consumption and state of charge (SoC) in the supercapacitor.
- Control of Regenerative Braking: Retrieves energy wasted during the braking process in the vehicle, recharges the supercapacitor, and preserves energy for use at a later time.

In order to achieve model transparency and determine the applicable range of the new portfolio against modeling assumptions, all parameter values for each system component were sourced from either the manufacturer's datasheets or established literature for that specific component(s). The collection of models has been created with a system-level energy management (rather than detailed electrochemical dynamics) perspective. The PEM fuel cell, power converters, traction motor, and ultracapacitor models—along with their associated modeling parameters and values as well as their sources, classifications, and whether they were identified/assumed/tuned parameters—are shown in Table 2.

This study attempted no parameter identification or tuning through experimentation. (For example, tuned parameters are limited to the bounds on optimising parameters adjusted by the application of a multi-objective genetic algorithm). Model confidence was measured through consistency analysis and benchmarking against known operating ranges reported in literature.

Established electric vehicle and power electronics literature was used to define the parameters for the DC/DC converter(s), DC/AC inverter(s), and traction motor; see Table 2 for these parameters.

Table 1. Comparison between the proposed method and existing GA/MOGA-based EMS studies for

Ref	EMS / Optimization Method	Objectives	Energy Storage	Driving Cycles	Constraints	Optimization Scope	Validation Type	Reported Quantitative Results
Guo *et al.*, 2025 [17]	GA-optimized Fuzzy EMS	Min equivalent H_2 consumption, SoC stability	FC + Battery	Standard cycles	SoC limits, power balance	Control parameters only	Simulation	−16.55% H_2 vs GA-EMS, −40.50% H_2 vs traditional fuzzy EMS
Yang & Wang, 2025 [18]	GA-based ECMS	Fuel economy, durability	FC + Battery	Standard cycles	SoC constraints	Control parameters only	Simulation	Fuel consumption ↓ 17.6% (UDDS), 9.7% (HWFET)
Zhou *et al.*, 2019 [19]	GA-optimized EMS	Minimize fuel consumption	FC + Battery	UDDS, HWFET	SoC & power	Control parameters	Simulation	~40% improvement in hydrogen utilization
Nasri & Gasbaoui, 2017 [12]	Neuro-fuzzy EMS	Traction safety, efficiency	EV hybrid	Urban cycles	Stability constraints	Control only	Simulation	Performance & stability improvement (qualitative)
Tazerart *et al.*, 2015 [20]	DTC-based control	Loss minimization	EV/FCV	Urban	Motor constraints	Control only	Simulation	Energy loss reduction (qualitative)
Hu *et al.*, 2021 [21]	Fuzzy-logic-based EMS considering SOH	Minimize hydrogen cost and fuel cell degradation	PEMFC + Battery	UDDS, NEDC, HWFET	SoC limits, SOH constraints*, power balance	Control parameters only	Simulation	Hydrogen cost reduction up to 13.76%, degradation cost reduction ≈ 7.9%
Mazouzi *et al.*, 2024 [22]	Comprehensive fuzzy EMS	Improve fuel utilization and FC efficiency	PEMFC + Battery	Standard driving cycles	SoC limits, power balance	Full fuzzy rule and membership optimization	Simulation	28.5% improvement in fuel utilization, 13% reduction in low-efficiency FC operation
This work	MOGA-based EMS + sizing optimization	Min H_2 + SoC balance + FC sizing	FC + Ultracapacitor	Standard + real Algerian route (OU12-ANN23)	SoC, power, sizing, regenerative constraints**	Control + component sizing	Consistency validation + benchmarking	Up to 30% H_2 reduction, robust convergence, SoC stability

*SOH constraints are introduced to limit operating conditions that accelerate fuel cell degradation and long-term performance loss. ** Regenerative braking constraints are applied to prevent overcharging and ensure stable energy recovery during deceleration.

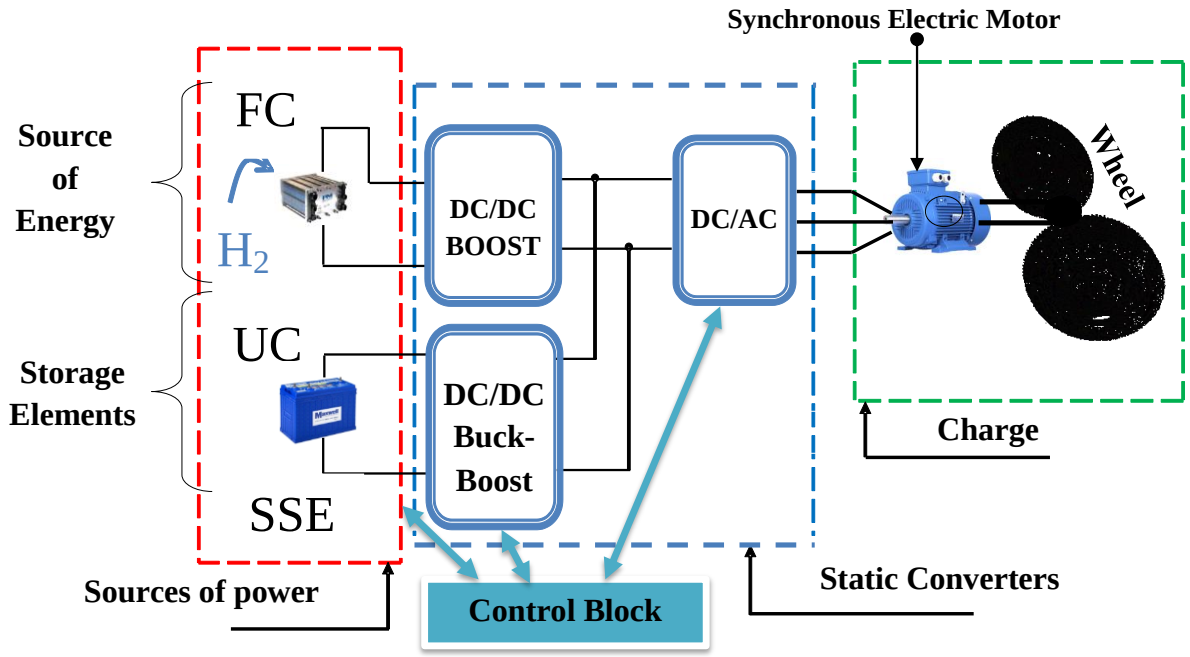

Figure 1. Structure of a fuel cell vehicle

Table 2. System Model Parameters, Sources, and Assumptions

Component	Parameter	Value	Unit	Source	Parameter Type
PEMFC	Operating temperature	80	°C	Manufacturer datasheet (Ballard) [23]	Assumed
PEMFC	Number of cells	125	–	Manufacturer datasheet [23]	Identified
PEMFC	Stack nominal voltage	48	V	Manufacturer datasheet [23]	Identified
PEMFC	Relative humidity	90	%	Literature [24, 25]	Assumed
PEMFC	Catalyst loading	0.3	mg/cm²	Manufacturer datasheet [23]	Identified
DC/DC Converter	Efficiency	95	%	Literature [26, 27]	Tuned
DC/AC Inverter	Efficiency	96	%	Literature [28, 29]	Assumed
DC/AC Inverter	Switching frequency	10*	kHz	Literature [28]	Assumed
Traction Motor (PMSM)	Rated power	75	kW	Literature [30]	Identified
Ultracapacitor	Capacitance	1500	F	Manufacturer datasheet [7]	Identified
Ultracapacitor	SoC operating limits	25–95	%	Manufacturer datasheet [7]	Identified

* Inverter switching frequency is the rate (typically 2−20 kHz) at which semiconductor switches (IGBTs/MOSFETs) turn on and off to convert DC to AC using Pulse Width Modulation (PWM). Higher frequencies improve output power quality and allow for smaller components, but increase heat, switching losses, and electromagnetic interference (EMI).

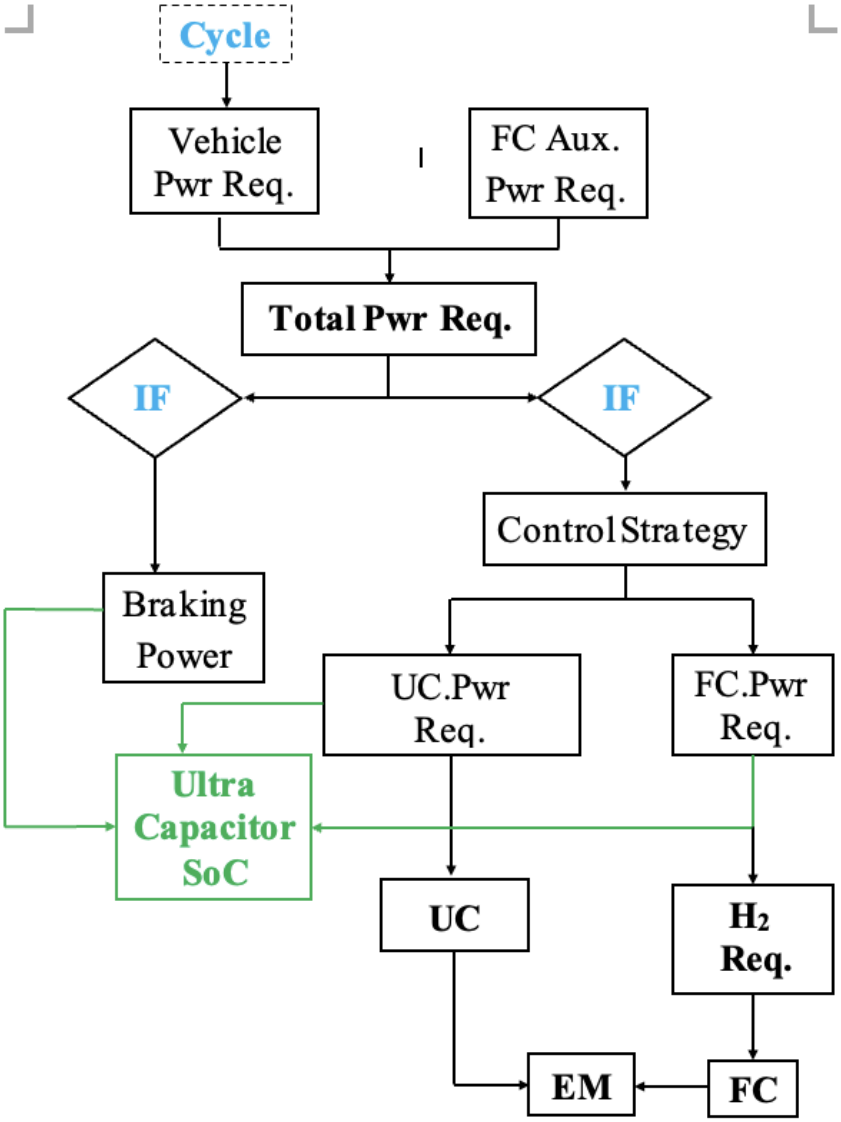

Figure 2. Flowchart of the simulation by Matlab/Simulation

These parameters are not based on experimental data but rather were chosen as representative of realistic and widely accepted values for fuel cell vehicle applications.

3. System Configuration

A fuel cell vehicle (FCV) utilizes a hydrogen-driven fuel cell and a Maxwell ultracapacitor [7], wired in parallel. Power flow is controlled through a control strategy, and the system connects to an electric motor through a DC/DC converter and a DC/AC inverter. During a demonstration of accelerating to 100 km/h in a total of 12.5 seconds, the fuel cell powers the electric motor while storing energy in the ultracapacitor device if the stored energy device level falls below the specified upper threshold. Regenerative braking also charges the ultracapacitor, ensuring efficient energy use during acceleration and deceleration.

4. Flowchart of the Simulation Code with Matlab/Simulink

The energy control strategy in the FCV, which has been modeled in Matlab/Simulink, includes an important role for the supervisor located in the motor controller. The supervisor coordinates energy flow between the fuel cell (FC) and the ultracapacitor, which allows for rapid acceleration and energy recovery during braking to promote overall energy efficiency.

The control strategy incorporates a key assumption that negative power corresponds to braking during deceleration, which can be recovered additively through regenerative braking. The ultracapacitor charging effectiveness is included in the energy stored during regenerative braking. Power requests include aerodynamic drag, rolling resistance, grade force, and inertial components. The simulation flow is depicted in Figure 2.

The vehicle's instantaneous power needs were determined using a retrograde model for a predefined driving cycle. The simulation utilized input and output variables, and the control strategy parameters were as follows:

- Input parameters: η, N, A_{FC}, UC_{SoC_Min}, UC_{SoC_Max}, Acc
- Output parameters: H_2, FC_use, UC_energy, UC_use

Definitely, the basis of the control strategy is to minimize hydrogen usage or to keep the so-called state of charge (SoC) of the energy storage device within acceptable limits. This control strategy aims to optimize power distribution in a hybrid powertrain for fuel efficiency and satisfactory operating conditions. To achieve this, the optimization problem can be stated as finding an optimal control law or power split parameter that minimizes hydrogen use over the complete driving cycle.

To achieve this, a cost function is defined, which quantifies the objective. Accordingly, the hydrogen consumption minimization problem is formulated as:

$$C_f = \int_{t=0}^{t=final} \dot{m_f} dt \quad (1)$$

Where: $\dot{m_f}$ is the flow rate of hydrogen consumption, and thus, the cost function C_f is the amount of hydrogen consumed over the driving cycle period from time $t = 0$ to time $t = t_{final}$.

The other aspect of the optimization is the SoC of the ultracapacitor stack, which can be accounted for as a constraint on the optimization problem.

Operational limitations are applied to the optimization problem to guarantee component protection and physical viability:

$$UC_{SoC}^{min} \leq UC_{SoC}(t) \leq UC_{SoC}^{max} \quad (2)$$

$$P_{FC}^{min} \leq P_{FC}(t) \leq P_{FC}^{max} \quad (3)$$

$$P_{UC}^{min} \leq P_{UC}(t) \leq P_{UC}^{max} \quad (4)$$

$$dP_{FC}/_{dt} \leq {}^{dP_{FC}}/_{dt}max \quad (5)$$

The optimization framework treats vehicle dynamics and driving cycle profiles as fixed inputs, while the parameters η, N, A_{FC}, UC_{SoC_min}, and UC_{SoC_max} are treated as decision variables. In Section 7, the corresponding optimization settings and the numerical bounds of these decision variables are described.

The formulation provides the basis for generating a multi-objective genetic algorithm as described in Section 7, as well as making sure that this energy management strategy and its implementation are able to be replicated completely.

In addition to being able to maximize the fuel efficiency of the powertrain, optimization techniques can also be used to size the vehicle components [10].

5. Power System

The energy system in an FCV consists of a two-source energy system—the primary energy source is the fuel cell (FC), and the secondary energy source is an ultracapacitor. The FC provides the necessary power to satisfy the demand for permanent energy, while the ultracapacitor provides power to satisfy rapid acceleration and energy recovery during braking. Therefore, the total electrical power accessible to the vehicle is determined by the sum of the power from the fuel cell (P_{FC}) and ultracapacitor power (P_{UC}).

$$P_{EM} = P_{FC} + P_{UC} \quad (6)$$

5.1 Fuel Cell Model

We utilize a fuel cell (FC) model based on empirical equations reported in the literature [24, 25], which is analyzed under steady-state operating conditions with constant relative humidity and without explicit limitations from chemical reaction kinetics. The adopted modeling approach is suitable for system-level energy management and optimization studies. The relevant operating parameters include a fuel cell temperature of 80 °C, a stack composed of 125 cells (N_{cell}), a relative humidity of 90% at the electrodes, a nominal stack voltage of 48 V, and a platinum catalyst loading of 0.3 mg/cm². Recent industrial developments indicate that advanced catalyst supports can significantly reduce platinum usage without performance degradation. In particular, Ballard Power Systems has demonstrated that carbon silk-enhanced catalysts enable a reduction in platinum loading by approximately 30% while maintaining comparable performance levels [23].

Based on Faraday's law, the mass flow rates of hydrogen and oxygen are computed as functions of the fuel cell current needed to meet the power demand:

$$\dot{m}_{H_2} = M_{H_2} * \frac{I_{FC}}{2F} \quad (7)$$

$$\dot{m}_{O_2} = M_{O_2} * \frac{I_{FC}}{4F} \quad (8)$$

Where M_{H_2} and M_{O_2} represent the molar masses of hydrogen and oxygen, respectively, F is Faraday's constant, and $\dot{m}_{H_2}$ and $\dot{m}_{O_2}$ denote the corresponding mass flow rates.

To improve the efficiency of the water removal process from the cathode channels of a PEMFC, an air excess ratio (ε) has been implemented. The ε value used in this research, 2, is in accordance with previous practice in PEMFC modeling studies and represents a stable condition for water removal [31].

5.1.1 PEMFC Voltage Model

The output voltage of a single PEM fuel cell is expressed as the difference between the reversible open-circuit voltage and the voltage losses associated with irreversible electrochemical phenomena. Accordingly, the cell voltage is given by:

$$V_{FC} = E_{rev} - V_{act} - V_{ohm} - V_{conc} \quad (9)$$

Where E_{rev} represents the reversible Nernst voltage, and V_{act}, V_{ohm}, and V_{conc} denote the activation, ohmic, and concentration losses, respectively.

The Nernst equation, which considers the temperature and reactant partial pressure, is used to calculate the reversible voltage. Activation losses are calculated using the semi-empirical formulation of the Tafel equation, and ohmic losses are calculated based on the resistance of the membrane, which is affected by the thickness, conductivity, and active area of the membrane. Concentration losses are modeled with a logarithmic equation to consider the effect of mass transport limitations at high dense current [32]. The methods described above are very commonly applied in PEMFC device models to optimize energy management studies with a reasonable degree of accuracy.

5.1.2 Stack Power and Efficiency

To determine the total voltage of a stack of fuel cells, you take the single cell voltage and multiply it by the number of cells in series. The electrical output from a fuel cell stack can be expressed as follows:

$$P_{FC} = V_{cell} \cdot N_{cell} \cdot I_{FC} \quad (10)$$

A fuel cell is efficient when it produces power with a high electrical output in relation to its chemical fuel (or hydrogen) input. A clear relationship between conditions under which fuel cells are operated, the output power generated, and how much hydrogen has been consumed can help in optimizing multiple objectives associated with operating fuel cell vehicles.

5.1.3 Modeling Assumptions and Scope

In order to optimize computation efficiency, a stationary-model fuel cell model has been created based on a polarized current curve. This type of modeling is typically used in energy optimization studies where the focus is on analyzing and forecasting long-term energy and fuel consumption patterns. To achieve stable operating conditions and maintain sufficient membrane hydration throughout the entire drive cycle, a constant ambient humidity level of 90% has been used.

While variations in humidity and electrochemical effects will affect performance during transients, the current study does not address these variables. The modeling method utilized represents a physically and computationally efficient representation of a fuel cell system and is therefore appropriate for multi-objective optimization for both standard and real-world driving conditions.

5.2 Ultracapacitor Model

In Table 3, the characteristics of the simulated ultracapacitor are mentioned, which is the Maxwell BCAP1500 [7]. The use of an ultracapacitor is especially beneficial if the power brake has to be restored. The reason ultracapacitors are used in vehicle setups is their high specific power rate and their ability to accept full recharge in a very short time, which leads to improved vehicle efficiency and energy economy.

5.3 The Auxiliary Components

The power that the FC system provides for the load is not 100% available. Some is used to drive auxiliary systems that are essential for operation. This system is made up of the compressor (Pcpm), the pump (Ppmp), and the radiator fan (Pradi) and is referred to as the fuel cell system.

Table 3. Characteristics of an ultracapacitor [7]

UC parameters	Unit	Values
Weight	g	280
Dimension	L (±0.3mm) × D1 (±0.2mm) ×D2 (±0.7mm)	85 × 60.4 × 60.7
Operating temperature	°C	-40 to 65
Rated capacitance	Farad (F)	1500
Energy density	Wh/kg	5.4
Power density	W/kg	6600
Package capacity	Ah	45
Package voltage	V	2.85
Current Rating	A	97
Life	Hours Or Cycle	1500 Hour, 1000000 Cycle

The FC system comprises four main circuits

Hydrogen Circuit (Closed Circuit)

- Supplies gaseous hydrogen to the anode
- Hydrogen remaining after the heat pump outlet can be recirculated by a pump.

Air Circuit (Open Circuit)

- It involves a compressor injecting air into the cathode to provide oxygen for the fuel cell.

Cooling Circuit (Thermal Management Circuit)

- The heat generated by the fuel cell includes a significant portion related to losses, which can exceed 50% of the total burn losses.
- The ambient temperature differences between the fuel cell and air are not significant; therefore, large heat exchangers must be utilized. This is very important in automotive applications.

Water Circuit (Water Management Circuit)

- Incoming gases (air and hydrogen) humidify the membranes through the water circuit.
- Water contributes to fuel cell cooling as it passes through the heat exchanger.

$$P_{aux} = P_{cpm} + P_{pmp} + P_{radi} \quad (11)$$

The air compressor is the main auxiliary component that uses the most energy in the fuel cell system, making it critical in defining the performance of overall system efficiency [33]. The power needed by the air compressor, calculated theoretically using isentropic gas compression, can be expressed as follows:

$$P_{cpm} = C_{sp} \cdot \left(\frac{T_{atm}}{\eta_{cpm}}\right)\left[\left(\frac{p_{air}}{p_{atm}}\right)^{\frac{\lambda-1}{\lambda}} - 1\right] \cdot \dot{m_{air}} \quad (12)$$

Where:

C_{sp} : The specific heat capacity

η_{cpm}: The compressor's efficiency

T_{atm} : The atmospheric temperature

ρ : The partial pressure

λ : The specific heat ratio

$\dot{m}_{air}$: Mass flow rate of air

The power output circuit of the fuel cell system may include various power conditioning systems, such as DC-DC converters or inverters. These systems manage the electrical output of the fuel cell system so that it is suitable for either the load or electrical system. The net power available for the vehicle is derived by subtracting the power consumed by auxiliary components (P_{aux}) from the total gross power (P_{Total}).

$$P_{FC} = P_{Total} - P_{Aux} \quad (13)$$

Current density (i) in fuel cells is defined as the current per unit area of the membrane. Current density can be defined in terms of area relating both the total current and the active area of the membrane:

$$i = \frac{I}{A_{FC}} \quad (14)$$

Where: i is the current density (A/cm^2), I is the total current (A), and A_{FC} is the membrane active area (cm^2).

6. Control Strategy

The energy management strategy presented emphasizes the fuel cell (FC) as the main energy source, selecting it on account of its high efficiency. The ultracapacitors will be used as a buffer to manage peak power. Ultracapacitors have higher power density and are thus used to assist the FC when there is an excess power demand above that generated by the FC.

This dynamic power distribution system operates as follows:

The FC will respond to a request for power initially. If demand exceeds FC capability, ultracapacitors will deliver supplemental power. The ultracapacitors are designed for long-term use and continuous duty; hence, they will be maintained at a given state of charge (SoC). The ultracapacitors will be recharged according to two principles:

- FC Surplus Energy: When the FC produces excess energy (i.e., beyond that consumed while operating the vehicle), that energy is used to charge the ultracapacitors.
- Regenerative Braking: When the vehicle decelerates from motion, it can harness energy that would be wasted in a normal braking event to charge the ultracapacitors.

This approach permits effective management of energy since energy can be conserved from the fuel cell while ultracapacitors are effective in controlling sudden transients. This will allow both being at the peak energy efficiency and, if needed, continuing the operation of the vehicle while managing energy effectively through a range of driving scenarios.

Figure 3 illustrates the power management strategy for the hybrid PEMFC and ultracapacitor system. Essentially, it determines where to draw power from based on instantaneous vehicle demand and the state of charge of the ultracapacitor. A set of thresholds for the ultracapacitor's SoC is predetermined so that the system knows what to do when the SoC hits those thresholds (either one or both thresholds). After the lower SoC threshold is breached, the fuel cell is turned on to compensate for the power draw from the electric load on the vehicle and, subsequently, the ultracapacitor.

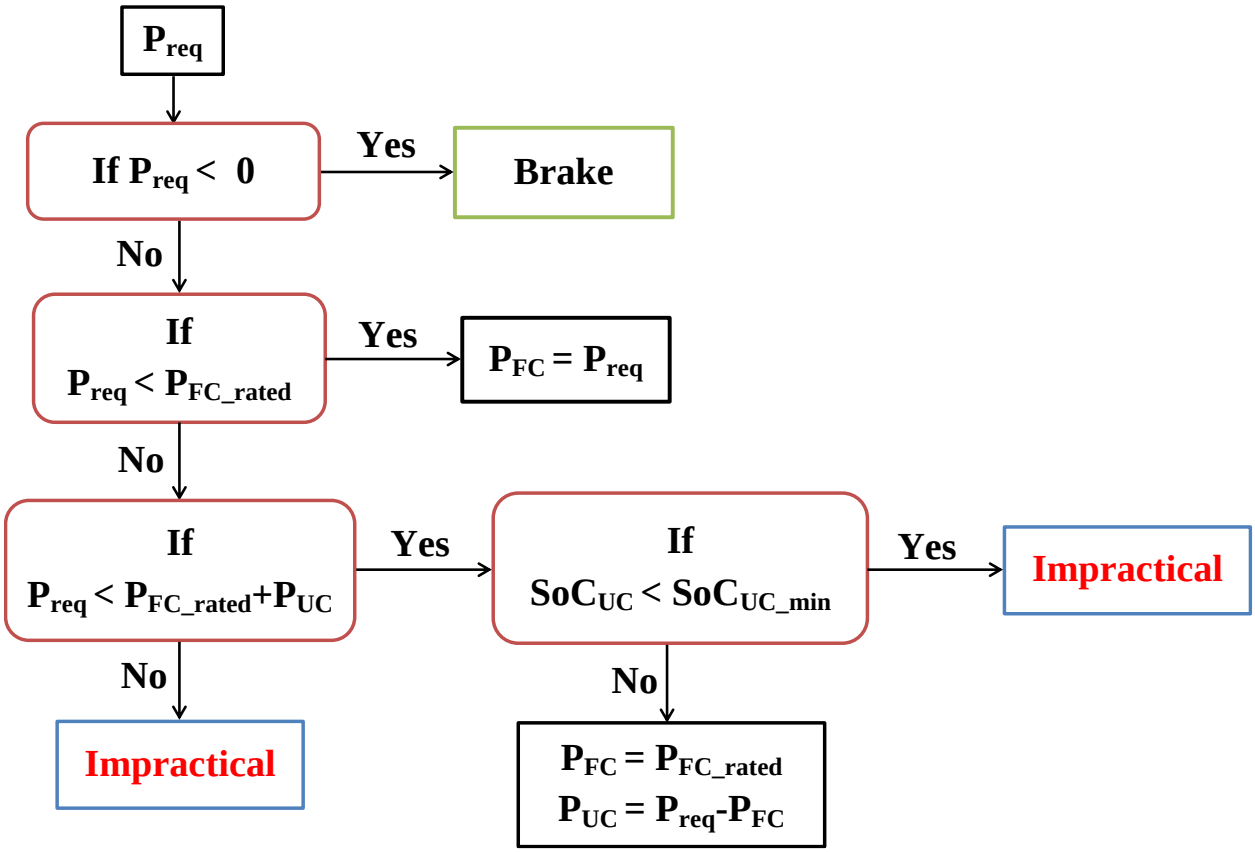

Figure 3. Control Strategy

Once the SoC rises above the upper limit, the fuel cell will reduce power (or shut off entirely), and the ultracapacitor will supply the entire power load. This electricity feedback loop from the fuel cell, contributes to providing balance, preserving system components, and maximizing the efficiency of hydrogens use in the vehicle. Each of those variables and parameters are to be optimized in concert, so that the MOGA optimization process returns a design that is optimally functioning.

6.1 Driving Cycle

A driving cycle is a number of data points that represent a vehicle's speed and acceleration over a specific time period and can be used to illustrate real driving conditions. Transient driving cycles are those that undergo a lot of acceleration and deceleration, while modal driving cycles consist of fixed speed intervals. The NEDC, WLTP, FTP, and Japan's 10-15 cycles are examples of test cycles that are typically used when assessing vehicle performance. Test cycles in general are the means of assessing all categories for measuring vehicle performance, including fuel economy, CO2 emissions, and performance measures.

In designing a fuel cell vehicle that utilizes ultracapacitors, the intent is to reduce the overall fuel consumption throughout a predetermined driving schedule, referred to as the driving cycle. The charge-sustaining rationale prohibits the depletion of an ultracapacitor and is monitored through the state of charge (SoC). The control strategy will be executed using the evaluation of deceleration status.

The change in acceleration/deceleration will use a threshold that they will operate within the interval of [-0.79; 0] m/s² to represent when the ultracapacitor has to recharge the ultracapacitor by regenerative braking when decelerating. For simulation purposes, the following driving cycles will be used: NEDC, UDDS, FTP, HWFET, and OU12-ANN23, each of which will represent a separate driving cycle.

- NEDC: European cycle for emissions and fuel economy, average speed of 33.21 km/h
- UDDS: an urban cycle that replicates driving conditions in cities at an average speed of 31.51 km/h.
- FTP: EPA cycle for city driving, with a 25.82 km/h average speed.
- HWFET: US EPA cycle for highway fuel economy evaluation, average speed of 77.58 km/h
- OU12-ANN23: Represents real-world driving in the Ouenza-Annaba region, with an average speed of 88.35 km/h.

Figure 4 shows the speed profiles for the five driving cycles considered in the simulations and optimizations presented in this paper

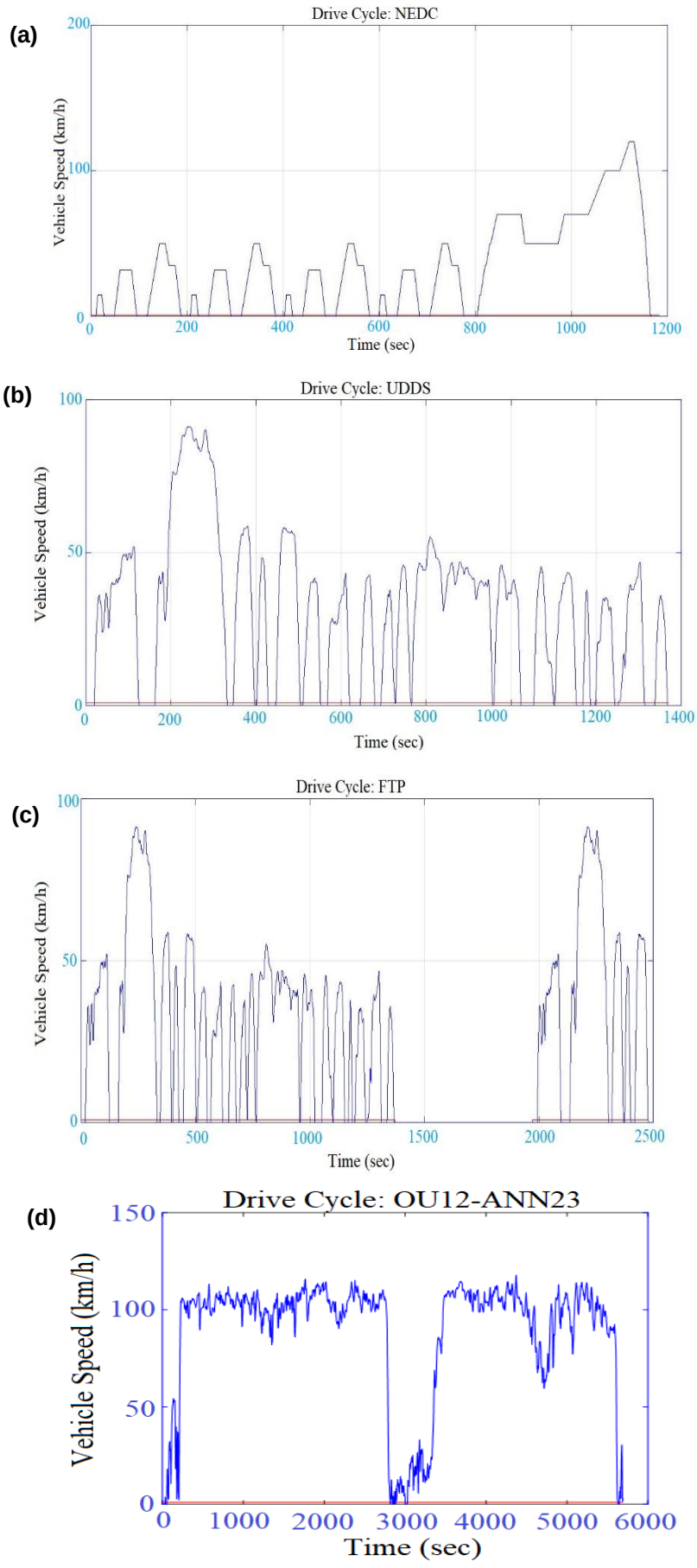

Figure 4. The different driving cycles we used in this study: **(a)** NEDC, (b) UDDS, **(c)** FTP, **(d)** HWFET, and **(e)** CYC_OU12-ANN23, which is a real-world driving cycle from Ouenza-Annaba.

- The New European Driving Cycle (NEDC), which exhibits relatively smooth acceleration and braking patterns representative of typical urban driving conditions.
- The UDDS cycle, which has a more dynamic, aggressive, high-acceleration profile that is representative of urban driving.
- The FTP-75 cycle, which represents the stop-and-go conditions that can be found in urban areas in the US.
- The HWFET cycle, which simulates steady-speed highway conditions with minimal braking.
- The real-world Algerian cycle (OU12-ANN23), which was collected along the route between El Ouenza and Annaba. This driving cycle represents a typical rural and urban mixed cycle with elevation changes, stops, and durations.

Beyond their speed–time profiles, these driving cycles exhibit distinct acceleration and deceleration patterns that directly affect transient power demand and energy distribution between the fuel cell and the ultracapacitor. Urban-type cycles (NEDC, UDDS, and FTP) are characterized by frequent stop-and-go behavior, enabling effective regenerative braking and short-term power buffering by the ultracapacitor. In contrast, the HWFET cycle involves smoother high-speed operation, resulting in a more sustained load on the fuel cell system. The combined route OU12–ANN23 will face unique energy management challenges, as it will include urban traffic congestion, intercity driving, and hilly surges of energy use. Therefore, this is a test of the robustness of the energy management system in a realistic environment.

One of the main reasons the Ouenza-Souk Ahras-Annaba (OU12-ANN23) route was chosen is because it is representative of a well-travelled corridor that connects universities/academic institutions and several urban centers located in northeastern Algeria. The OU12-ANN23 route is characterized by daily peak traffic patterns, which include urban congestion, intercity trips, and variable road profiles along its length. Because of the frequency and consistency of traffic on this route, it is possible to use the driving data collected along this route as a reasonable representation of the actual, repeatable operating conditions that occur on this route, and hence this route is suitable for use as the base or reference route for conducting energy management studies. Therefore, if the methodology proposed in this research is used to establish the OU12-ANN23 route as the reference case study for energy management studies, then it would also be reasonable to expand and generalize the methodology for use on other roads with similar traffic and topographical characteristics.

6.2 Path-Driving Cycle

In the fuel cell vehicle study, the driving route runs from Ouenza to Souk Ahras to Annaba, Algeria, which is a total distance of about 150 kilometers. If everything is normal, the total duration will be approximately 2 hours and 50 minutes. There have been a number of stops included in the course. The first speed slowdown is when entering Mechroha, which is approximately 71.5 km from Ouenza. Speed bumps and stop signs in Mechroha all contribute to the reduction of travel speed. As illustrated in Figure 5, the driving cycle begins in Ouenza and passes through Souk Ahras before reaching Annaba.

Figure 5. Illustrates the intended route for the driving cycle carried out during the fuel cell vehicle study (Ouenza–Souk Ahras–Annaba, ≈ 150 km.

7. Optimization Problem Formulation and MOGA Settings

This research will use a Multi-objective Genetic Algorithm in MATLAB/Simulink to develop an Energy Management Strategy for optimizing the hybrid fuel cell vehicle powertrain and its most critical sizing parameters. The optimization is structured to minimize the total hydrogen usage while maintaining stable operation of the ultracapacitors and ensuring the hybrid's operation is feasible under all possible conditions (driving cycles).

7.1 Objective Functions

The optimization problem was formulated as a bi-objective optimization problem, through the unification of the following two sub-criteria into one objective function:

Objective 1: Minimize total hydrogen consumption over the driving cycle

$$f_1 = \int_0^T \dot{m}_{H_2}(t)dt = \min(H_2)\,[g/100\,km] \quad (15)$$

Objective 2: Maximize ultracapacitor SoC sustainability

$$f_2 = \max\left(soc_{UC}^{final} - soc_{UC}^{initial}\right)\ [\%] \quad (16)$$

Although it lacks a clear objective function, the fuel cell's efficiency can still be enhanced through Pareto optimization by optimizing the operating parameters (e.g., pressure) for a fuel cell power generation system while reducing hydrogen consumption and maintaining the functioning of the sustainable energy storage system.

7.2 Decision Variables

The decision vector is defined as:

$$x = \left[\eta_{FC}, N_{FC}, A_{FC}, SoC_{UC}^{min}, SoC_{UC}^{max}, dec_a\right] \quad (17)$$

Where: dec_a is deceleration threshold for regenerative braking activation.

Table 4. Range value (Optimization parameters - Min/Max)

Parameters	Min	Max
η (%)	40	50
N	1	6
A (cm^2)	400	550
SOC_{UCmin} (%)	20	40
SOC_{UCmax} (%)	75	95
Acc (%)	10	90

7.3 Variable Bounds

The optimization bounds are summarized in Table 4.

7.4 Constraints

The optimization is subject to the following constraints:

- Power balance constraint:

$$P_{dem}(t) = P_{UC}(t) + P_{FC}(t) \quad (18)$$

- Fuel cell power limits

$$0 \le P_{FC}(t) \le P_{FC}^{rated} \quad (19)$$

- Ultracapacitor SoC constraint:

$$SoC_{UC}^{initial} \le SoC_{UC}^{final} \quad (20)$$

- Hydrogen consumption constraint:

$$H_2 \le 300\ g \quad (21)$$

There are additional implicit constraints on the ultracapacitor, which include the charge and discharge limits; the fuel cell, which involves both the maximum and minimum power output; and the dynamic response limits imposed by the powertrain simulation using Simulink.

7.5 MOGA Configuration

The multi-objective genetic algorithm that was developed and implemented in MATLAB used the optimization toolbox within the following configuration of application:

- Population size: 100
- Number of generations: 150
- Selection method: Tournament selection (size = 2)
- Crossover operator: Simulated binary crossover
- Crossover fraction: 0.8
- Mutation operator: Polynomial mutation
- Mutation rate: 0.05

Elitism: Enabled (Pareto front preservation)

- Termination criterion: Maximum number of generations
- Number of independent runs: 5 (All of the previously listed Pareto fronts and the best parameterization solution from each of the five independent optimization trials produced the same compromise solution consistently).
- Initial population: Randomly generated within predefined bounds
- Random seed policy: Random initialization to avoid local optimal (Different random initializations were used for each independent trial and within each independent experiment to

increase solution diversity and help avoid local optima due to premature convergence through the use of a sequential fixed random seed approach).

- Average computational time: Approximately 2–4 hours per driving cycle on a standard workstation

The designated settings were determined to enable stable convergence of the Pareto front throughout all driving cycles to provide reliable and consistent optimization outcomes.

8. Results and Discussion

The obtained results are consistent with previously reported studies on fuel-cell hybrid electric vehicles employing optimized energy management strategies. Similar trends regarding hydrogen consumption reduction and fuel cell load smoothing have been observed in rule-based and optimization-based approaches reported in the literature [17, 34], and [35].

In an effort toward replicability and transparent evaluation, five distinct driving cycles with different dynamic characteristics were used in this research: NEDC, UDDS, FTP 75, HWFET, and a real-world Algerian route (OU12-AN23). Each of the five cycles was selected because it represents urban, mixed, and highway driving conditions and originated from regulatory databases that made the data publicly available; on the contrary, the Real World Route was created from on-the-road measurements between Ouenza and Annaba. The total distance of the New European Driving Cycle (NEDC) is 10.93 km, and it has a duration of 1184 s; the average speed is 33.21 km/h, while the maximum speed is 120 km/h, which is classified as low- to moderate-dynamic urban driving with many stops. On the other hand, the Urban Driving Dynamics Simulation (UDDS) is 1369 s and 11.99 km and displays higher levels of transience (1.48 m/s² peak acceleration) and has 17 stops; as such, it is representative of congested urban driving conditions. Finally, the Federal Test Procedure (FTP-75) represents a continuation of the UDDS by exhibiting the same type of behavior over a longer period of time (2477 s) and distance (17.77 km), as well as through repeated cycles of acceleration/deceleration and idle throughout the drive cycle; these characteristics create continuous loads on the hybrid powertrain. Furthermore, the HWFET Cycle (765 s, 16.51 km) represents a consistently high-speed operation (77.58 km/h) with minimal stopping as it relates to an efficiency-based highway driving mode. The Real World OU12–ANN23 route (5692 s, 139.72 km) includes real-world traffic behavior and significant variations in speed, as well as upward and downward road slopes of 7.5% maximum and 7.9% maximum, respectively. The Real World OU12–ANN23 Route offers a real-world geographical and operational validation beyond de-junction biometrics created from urban use. Consistency of the parameters used in the simulations (i.e., mass M_{veh}=1740kg, drag coefficient, frontal area, and rolling resistance) was upheld between the different cycles to ensure a fair evaluation of each simulation. While the real-world route would incorporate road grade profiles, the standardized cycles were created to include only flat grades (0% grade). These characteristics make it possible to recreate the simulation framework completely and make it possible to compare the optimization results across studies. Table 5 provides a summary of each driving cycle's characteristics.

The Pareto fronts created utilizing five different driving cycles (i.e., FTP, UDDS, NEDC, OU12-ANN23, and HWFET) are illustrated in Figure 6. The Pareto fronts show how hydrogen consumption is balanced against system performance for each driving cycle. The UDDS driving cycle demonstrates that despite its greater total energy consumption when compared to NEDC, the frequent slowing down during the UDDS driving cycle provides for effective regeneration of the energy used by the ultracapacitor, thereby increasing fuel efficiency. These observations are consistent with findings reported in previous FCV energy management studies operating under transient driving conditions [6, 13].

Table 5. Characteristics of the driving cycles used in this study

Cycle	Duration (s)	Distance (km)	Avg Speed (km/h)	Max Speed (km/h)	Stops	Idle Time (s)	Max Accel (m/s²)	Max Grade (%)
NEDC	1184	10.93	33.21	120	13	298	1.06	0
UDDS	1369	11.99	31.51	91.25	17	259	1.48	0
FTP-75	2477	17.77	25.82	91.25	22	360	1.48	0
HWFET	765	16.51	77.58	96.4	1	6	1.43	0
OU12–ANN23	5692	139.72	88.35	117.83	5	114	2.38	7.5

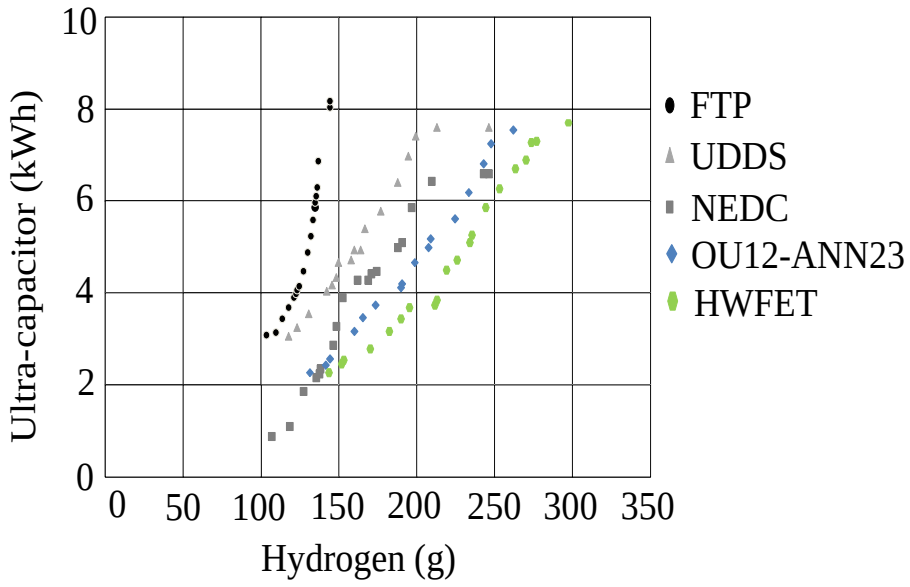

Figure 6. Representation of Pareto fronts based on the driving cycles

The driving cycle's dynamic properties, which are compiled in Table 6, have a direct impact on the Pareto-optimal solutions. In order to keep fuel cell operation close to efficient steady-state regions and lower hydrogen consumption, urban cycles like UDDS and FTP-75, which are marked by frequent stops, low average speeds, and high acceleration/deceleration rates, create Pareto fronts that favor increased ultracapacitor utilization. On the other hand, because of the lower transient power demand, quasi-steady cycles like HWFET, which have higher average speeds and fewer stop events (Table 5), generate more compact Pareto fronts where hydrogen reduction and efficiency improvement are more closely aligned. The real-world OU12–ANN23 route, whose duration, distance, speed range, and road grade statistics are reported in Table 5, exhibits a distinct Pareto behavior compared with standardized cycles. Its longer duration, higher average speed, and nonzero road grade require sustained coordination between the fuel cell and ultracapacitor, leading to Pareto solutions that converge toward balanced operating points. This smoother convergence indicates robust parameter adaptation under realistic and heterogeneous driving conditions.

The number of fuel cell stacks (N), fuel cell efficiency (η), and ultracapacitor state-of-charge limits (SoC_{UCmin} and SoC_{UCmax}) mainly govern how optimal solutions will be located along the Pareto front. The hydrogen consumed will increase with an increase in *N* and a decrease in *η*; however, with an increase in the range over which SoC of the ultracapacitor operates, the hydrogen consumed will decrease. Lower values for SoC_{UCmin} enable deeper utilization of the ultracapacitor, which reduces the amount of transient loading put on the fuel cell, leading to a better overall hydrogen economy. These trends have been identified across various optimization methods used within EMS for hybrid fuel cell vehicles (FCVs) [14, 15].

The parameters optimized through the execution of several different driving cycles appear to converge relatively similarly among the cycles, indicating that system-level constraints are more impactful in the optimization process than cycle-specific tuning. In particular, fuel cell efficiencies and ultracapacitor limits on state-of-charge (SoC) converge and stabilize within narrow ranges throughout the different optimized driving cycles. This suggests that the optimization algorithm consistently selects operating regions that avoid inefficient fuel cell transients while permitting ultracapacitors to buffer quick power changes and regenerative braking events. From the results, the generated Pareto front demonstrates an inherent trade-off between hydrogen use and overall system efficiency.

Generally less hydrogen is consumed when ultracapacitor utilization within the SoC constraint range is maximized; however, this increases regenerative energy capture while also increasing conversion losses and current stresses on both fuel cells and ultracapacitors. Fuel cells operated at a more stable region within their respective performance envelope tend to be more efficient, which generates less transient loss, but normally use more hydrogen as compared to the other driving cycles. The trade-offs reveal that the relationships observed by the Pareto front are intrinsic to the system-level interaction, not at all affected by specific driving cycle characteristics.

With regard to high-speed/higher power cycles like HWFET and OU12-ANN23, larger active area fuel cells are generally the best-performing option since both require longer running durations at higher average vehicle speeds (117.83 km/h for OU12-ANN23), thus calling for more consistent FC output. Additionally, there was an increase in the volume of hydrogen consumed by this cycle compared to lower speed highway cycles [6].

While the optimized parameter sets exhibit variability in their specific sets of Pareto-optimal from Table 6, the trends in convergence of each of the optimized sets appear similar across nearly all of the defined driving cycles. The differences in the maximum operating limits that may be allowed in some configurations (e.g., $SoC_{UCmin} \approx 27\%$ and $SoC_{UCmax} \approx 87\%$) to achieve maximum hydrogen savings in selected cycle types would create a large number of solutions that converge on moderate, stable operating limits for the remainder of the driving cycles. In these cycles, the efficiencies of the fuel cell have all converged on a typical range of 45–46%, and the active area of the fuel cells continues to generally remain within a range of approximately 400–425 cm^2. The results demonstrate that the variables associated with design and control identified through the MOGA-based model represent a design and control strategy that is resilient to the variability in driving styles that are encountered and that it optimally addresses the dual goals of hydrogen reduction and operational constraints.

The hydrogen reductions achieved through the MOGA-based energy management strategy can be interpreted with respect to the two separate analyses presented in Table 1. In Table 1, it was demonstrated that the hydrogen reductions provided by the proposed MOGA-based energy management strategy were at or above the upper limit of the reductions reported among existing studies utilizing GA/MOGA for energy management in FCVs. Previous studies utilized standardized driving conditions to evaluate the effectiveness of optimally controlling various system parameters; however, strong evidence provided from the MOGA-based energy management strategy indicates that fuel savings are obtainable using more realistic regional driving conditions and that the results support the reproducibility of the Pareto-optimal solutions achieved, thereby demonstrating that the observed hydrogen use reduction is consistent with other hydrogen savings found in the literature.

Table 6. Optimal input parameters for each driving cycle

Parameters	Driving Cycle				
	FTP	**HWFET**	**UDDS**	**NEDC**	**OU12_AN23**
Powertrain Components Inputs					
Fuel cell operating efficiency (η) (%)	46	45.55	46	45.50	45.50
Number of fuel cell stacks (N)	1	2	1	1	2
Fuel cell active area (A_{FC})	424	413	400	415	412
UC_SOC_MIN (%)	38	28	29	30	**27**
UC_SOC_MAX (%)	80	79.5	79.5	**87**	79.5
EM Output Power Max (kw)	60	60	60	60	60
System power density (W/kg)	276	276	276	276	276
Simulations Outputs					
Total Fuel Consumption (H_2) (g/100km)	**108.70**	139.80	116.40	116	126.20
Distance (km)	17.77	16.51	11.99	10.93	139.72
Time (s)	2477	765	1369	1184	5692
Max Speed (km/h)	93.25	96.40	91.25	120	117.83
Average speed (km/h)	25.82	77.58	31.51	33.21	88.35
Specific Fuel Consumption (g/km)	6.11	8.46	9.70	10.61	0.90
Specific Energy Consumption (MJ/100km)	73.32	101.52	116.4	127.32	10.8

Table 7. Utilization percentage of each storage system for the five cycles

Cycles	Storage System	
	Fuel cell (%)	**Ultracapacitor (%)**
UDDS	53	47
NEDC	54	46
FTP	67	33
HWFET	69	31
OU12-ANN23	70	30

The results of Table 6 illustrate how hydrogen consumption (minimization) is optimally balanced against operational constraints. The bolded values in this table are, therefore, the most representative of the Pareto-optimal solutions that will be discussed in detail.

To further analyse energy distribution, the utilization ratio of each energy source is calculated using Equation (20);

$$U_{ratio_i} = \frac{\int_{Cycle} P_i(t)dt}{\int_{Cycle} P_{FC}(t)dt + \int_{Cycle} P_{UC}(t)dt} \times 100 \quad (22)$$

Where Pi(t) represents the instantaneous power supplied by either the fuel cell or the ultracapacitor.

Table 7 provides utilization percentages associated with how much of the total energy demand was met by fuel cells. The range of contribution to total energy demand for the fuel cell is between 53% and 70%, depending on which driving cycle is used. Aggressive transient driving cycles, such as UDDS and NEDC, see more energy utilized from ultracapacitors because of the number of times they accelerate and brake within these driving cycles. These trends are consistent with hybrid energy storage behavior reported in the literature [12].

Fuel cell vehicles (FCVs) use substantially less specific energy than conventional types of vehicles. The configuration of the suggested FCV produces values ranging from 73 to 127 MJ/100 km. This energy reduction of approximately 40% is in comparison to the normal value of about 171.6 MJ/100 km that is available for vehicles powered by internal combustion engines (ICE). This improvement can be attributed to the higher efficiency of the drivetrain and the optimal use of the fuel cell power and hydrogen ultracapacitors, and it is consistent with research conducted previously on hydrogen propulsion systems [1, 3].

8.1 Energy-flow consistency and Pareto interpretation

The energy flow accounting presented in Table 8 also provides clarification regarding the physical origin of the Pareto trade-off that has been illustrated within Figure 6.

An energy balance restriction was imposed on each Pareto-optimal representing solution in order to assure the reported outcome's physical coherence. During an entire driving cycle, the traction energy requirement must meet the following:

$$E_{trac} = E_{FC} + E_{UC}^{dis} - E_{loss} \quad (23)$$

Where: E_{FC} is the amount of energy delivered by the fuel cell stack, while E_{UC}^{dis} is the amount of discharged energy from the supercapacitor. E_{loss} is the sum of losses caused by the DC/DC and DC/AC power converters and inverter losses. Energy from regenerative braking is initially stored in the supercapacitor, thus indirectly contributing to E_{UC}^{dis}. To eliminate non-physical energy exploitation, those solutions that performed outside of this balance were excluded from consideration for the Pareto set.

In addition to the metrics mentioned above for measuring performance, each combination of the fuel cell, ultracapacitor, and traction (driving) system can produce uniquely defined distributions of energy flowing through them from one device to the next. A summary of how much total energy was accounted for across the different driving cycles with all representative solutions found on the Pareto curves is presented in Table 8. Lower fuel-cell demand solutions are found at the far left side of the Pareto curve, where there was much greater use of regenerative braking energy compared with transient discharge of ultracapacitors, thereby resulting in lower overall fuel-cell usage. Solutions that were oriented toward maximizing the efficiency of the fuel cell had their fuel-cell stacks operating in a more stable and narrow capacity range while also reducing the potential to reuse regenerative energy.

An energy-flow analysis provides an explanation for the observed trade-off between the two areas of the Pareto curve and demonstrates that the shape and convergence of the Pareto curves result from legitimate physical mechanisms of energy transfer and not as an artifact of optimizing numerical values.

8.2 Baseline Comparison with Rule-Based EMS

A baseline rule-based control approach was implemented to validate the effectiveness of the proposed MOGA-based energy management strategy

The fuel cell provides the average power demand, while the ultracapacitor manages the transient power peaks during acceleration and recuperates braking energy during deceleration in this RB strategy. This type of control method is often cited in the literature for its simple configuration and ease of use [10].

Both methods were tested on an equal basis against four Standard Driving Cycles (NEDC, FTP-75, UDDS, and HWFET) and a real-world route in Algeria (OU12-ANN23). Performance between methods was compared based on the total amount of hydrogen consumed, the average power produced by the fuel cell, and how stable the SOC of the ultracapacitor was.

As reported in Table 9, the proposed MOGA-based EMS consistently outperforms the RB strategy across all driving cycles. Hydrogen consumption reductions range from 24% to 30.5%, while average fuel cell power demand is reduced by approximately 16–18%. As a result of these developments, the size of the stack could be smaller than before, and the efficiency of the entire fuel cell system will be increased as a result. Specifically, the hydrogen reduction is about 30% lower than

previous research has reported, and in some situations, it is more than this figure. As an example of optimal EMS strategies implemented in hybrid fuel cell (FC) and ultracapacitor (UC) systems; the published findings show hydrogen savings varying from 15% to 25% under standard driving cycles [2, 19]. The potential for improved overall hydrogen savings and performance from coordination between the two devices (FC and UC) while staying within the SoC constraints of the ultracapacitor consistently kept within ±5% of acceptable SoC limits would suggest that from an operational point of view, optimizing would be beneficial with respect to the reliability/stability of the overall system as well as the longevity (i.e., lifetime) of both the ultracapacitor and fuel cell.

Table 8. Energy Flow Accounting over Driving Cycles (Representative Pareto-Optimal Solutions)

Cycle	FC Energy (kWh)	UC Discharge (kWh)	UC Charge (kWh)	Regen Energy (kWh)	Converter Losses (kWh)	Traction Demand (kWh)
NEDC	4.62	0.88	0.95	0.92	0.33	5.17
UDDS	4.95	1.12	1.18	1.15	0.38	5.69
FTP	7.05	1.55	1.63	1.60	0.52	8.08
HWFET	6.35	0.62	0.66	0.64	0.44	6.53
OU12-ANN23	54.20	3.85	4.20	4.05	4.10	53.95

Table 9. Contrast comparison between Rule-Based (RB) and MOGA strategies

Driving Cycle	H_2 Consumption RB (g/km)	H_2 Consumption MOGA (g/km)	Savings (%)	Avg. FC Power RB (kW)	Avg. FC Power MOGA (kW)	Reduction (%)
NEDC	8.5	6.1	28.2%	34.0	28.5	16.2%
FTP-75	9.2	6.8	26.1%	36.5	30.4	16.7%
UDDS	7.8	5.9	24.4%	33.1	27.2	17.8%
HWFET	6.0	4.5	25.0%	29.5	24.5	16.9%
OU12–ANN23	10.5	7.3	30.5%	38.2	31.1	18.6%

Furthermore, the optimal SoC operating limits selected (as proposed in this research) are in accordance with many works found in the literature that suggested keeping the depth-of-discharge moderate in order to improve electrical recuperation capacity and protect FC and UC system integrity and longevity [3, 5].

The MOGA-based framework has a significantly broader application range and higher performance than other methods of RB in both standardized and real-world driving conditions. The potential future application of the MOGA-based framework for real-time applications, with the implementation of advanced control methodologies, such as model predictive control or reinforcement learning, is very promising. In this regard, a MOGA-based framework has the potential to be used for enhanced adaptability and robustness in environments of uncertain road conditions.

The hydrogen reduction and efficiency trends achieved have been consistent with other studies using GA/MOGA-based EMSs. In addition, when evaluated either in standardized or real-world driving conditions reported in the literature, the hydrogen reduction and efficiency trends show comparable or improved performance.

8.3 Model Validation and Consistency Analysis

Although experimental validation is beyond the scope of this study, the proposed hybrid FCV model and optimization results were validated through consistency checks and benchmarking against existing literature. First, the fuel cell polarization characteristics, efficiency range, and power response under dynamic driving cycles were verified to remain within commonly reported operating ranges for PEMFC-based vehicle applications. The optimized fuel cell efficiency converging around 45–46% is consistent with values reported in recent FCV energy management studies under transient operating

conditions [4, 6, and 13]. Specifically, the simulated voltage and efficiency levels remained within ±5–8% of ranges reported in comparable PEMFC vehicle studies.

In addition, the transient characteristics of fuel cell stack powers, fuel cell stack voltages, and system efficiencies were also physically rechecked during rapid load changes resulting from both acceleration and deceleration events and found to produce physically consistent results when subjected to dynamic operating conditions.

Furthermore, the energy flow balance between the fuel cell and ultracapacitor and traction system was monitored throughout all driving cycles to ensure they would all work together in a physically feasible manner. The final state of charge of the ultracapacitor remained at or above its initial value for all of the selected Pareto-optimal solutions; thus, indicating that energy was being used sustainably and not being depleted. This confirms that the optimization process does not exploit numerical artifacts or non-physical energy behavior to achieve hydrogen savings.

Furthermore, the observed trade-off trends between hydrogen consumption and ultracapacitor operating limits align with previously published optimization-based EMS approaches for hybrid FCVs, where moderate SoC operating windows lead to improved regenerative energy recovery and reduced hydrogen usage [10, 14]. Therefore, the convergence of optimal parameters across heterogeneous driving cycles provides indirect yet strong evidence of the validity of the proposed MOGA-based optimization framework.

Nevertheless, it is acknowledged that the absence of experimental or hardware-in-the-loop validation represents a limitation of the present work. Future research will focus on experimental validation and real-time implementation of the proposed strategy on a prototype FCV platform.

This validation step enhances confidence in the optimization outcomes and supports the applicability of the proposed framework under realistic driving conditions.

9. Conclusion

The proposed study presents an optimized energy management framework for hybrid fuel cell vehicles integrating a PEMFC and an ultracapacitor, using a multi-objective genetic algorithm. While most prior work has relied solely upon a standard driving cycle and assumption-based evaluation, the present study utilized the actual Algerian Driving Cycle (OU12-ANN23) and thus accounted for all aspects of local conditions, such as driver behavioral factors, traffic trends, speed fluctuations, and variations of energy demand based on traffic volumes. This approach increases the viability of this energy management system when applied in an actual and practical environment.

This research contributes significantly by providing a unified multi-objective optimization of both hydrogen consumption and the state-of-charge of ultracapacitors, which is used to determine the size of a fuel cell. The simulations indicate that this method can reduce hydrogen consumption by as much as 30% over many different types of driving but still allows the vehicle to achieve its performance levels while meeting the operating limitations of the hybrid vehicle powertrain. The similarities between the various optimized parameters obtained from the various simulations also validate the reliability of the proposed methodology.

In addition to enhancing performance, this effort also addresses important issues relating to cost efficiency, scalability, and sustainability of fuel cell vehicle powertrains. The framework takes into account realistic driving environments as well as component-level constraints, allowing for an understanding and integration of real-world energy management strategies with workable control schemes. As a result, the results of this work provide insights for designing and optimizing FCVs in the future, whether in developed or developing areas.

This work will provide a basis for future studies that include proof of the experiments, creating data based on several different energy management strategies, using energy models that are specific to different areas of the world, and designing more economical fuel cell systems. Such extensions would further enhance the practical deployment potential of optimized FCV technologies. Even though the new framework shows good performance, it must be recognized that the multi-objective genetic algorithm is a method of offline optimization, so it cannot be implemented directly in real-time because of the large amount of computations. However, the optimized solutions gained can be converted to reference maps or simplified control rules that are applicable for real-time use. Consequently, future investigations will concentrate on providing an experimental validation, hardware-in-the-loop implementation, and development of real-time control.

10. Perspectives and Future Research Directions

- Use of renewable energy: The sustainability of the fuel cell vehicle system can be enhanced, reducing reliance on hydrogen, by using solar or wind energy sources.
- Machine Learning Control Systems: By taking advantage of machine learning systems, the fuel cell vehicles would be able to adapt to driving parameters in real-time while in operation and

optimize energy management and control strategy.

- Real-life Testing: The extensive testing will increase the reliability of the fuel cell hybrid, and the data from the operation of actual fuel cell vehicles will support moving fuel cell vehicles from concept to commercialization, from part to system level.
- Halogen Storage: Modern storage methods using substances such as metal hydrides could increase cost, capacity, and safety in storing hydrogen.
- Innovative Ultracapacitors: Time-to-range performance could dramatically enhance with the introduction of new materials that increase the energy density of the ultracapacitor.
- Environmental Issues: Sustainability requires research into long-term parts of the life cycle of H_2 production and fuel cell vehicles.
- Cost Reduction: Future advances will also allow for materials and methods of producing fuel cell vehicles and hydrogen to become less expensive.

A second goal will be to improve the performance of next-generation fuel cell vehicles by making them more reliable, less expensive, and sustainable.

References

[1] O. Bethoux, Hydrogen Fuel Cell Road Vehicles and Their Infrastructure: An Option towards an Environmentally Friendly Energy Transition. Energies, 13(22), (2020) 6132. https://doi.org/10.3390/en13226132

[2] I. Oukkacha, (2019) Systemic approach for electrical management dedicated to transport applications using electrochemical storage systems. Ph.D. Thesis, Research Group in Electrotechnics and Automation of Le Havre, Normandy University, France. https://theses.hal.science/tel-03080962v1/document

[3] H.J. Lim, G. Kim, G.J. Yun, Durability and Performance Analysis of Polymer Electrolyte Membranes for Hydrogen Fuel Cells by a Coupled Chemo-mechanical Constitutive Model and Experimental Validation. ACS Applied Materials & Interfaces, 15(20), (2023) 24257–24270. https://doi.org/10.1021/acsami.2c15451

[4] S. Ahmadi, S.M.T. Bathaee, Multi-objective genetic optimization of the fuel cell hybrid vehicle supervisory system: Fuzzy logic and operating mode control strategies. International Journal of Hydrogen Energy, 40(36), (2015) 12512–12521. https://doi.org/10.1016/j.ijhydene.2015.06.160

[5] M.A. Biberci, M.B. Celik, Dynamic Modeling and Simulation of a PEM Fuel Cell (PEMFC) during an Automotive Vehicle's Driving Cycle, Engineering. Technology & Applied Science Research, 10(3), (2020) 5796–5802. https://doi.org/10.48084/etasr.3352

[6] C. Pan, S. Tao, H. Fan, M. Shu, Y. Zhang, Y. Sun, Multi-Objective Optimization of a Battery-Supercapacitor Hybrid Energy Storage System Based on the Concept of Cyber-Physical System. Electronics, 10(15), (2021) 1801. https://doi.org/10.3390/electronics10151801

[7] Maxwell Technologies, (2013) K2 series Maxwell ultracapacitors. 1015370.4 datasheet. https://www.mouser.fr/datasheet/2/257/Maxwell_K2Series_DS_1015370-4-1179730.pdf

[8] F. Tazerart, A. Azib, F. Kerrouche, T. Rekioua, Hydrogen fuel cell electric vehicles controlled by direct torque control (DTC) during low-speed operation. Journal of Renewable Energies. 27(1), (2024) 115 – 131. https://doi.org/10.54966/jreen.v27i1.1157

[9] F. Tazerart, F. Kerrouche, A. Azib, T. Rekioua, Improving efficiency through the optimization of energy losses in an induction machine for electric vehicle propulsion. Journal of Renewable Energies, 27(1), (2024) 67 – 80. https://doi.org/10.54966/jreen.v27i1.1158

[10] H. Pei, X. Hu, Y. Yang, X. Tang, C. Hou, D. Cao, Configuration optimization for improving fuel efficiency of power split hybrid powertrains with a single planetary gear. Applied Energy, 214, (2018) 103–116. https://doi.org/10.1016/j.apenergy.2018.01.070

[11] S.F. da Silva, J.J. Eckert, F.L. Silva, L.C.A. Silva, F.G. Dedini, Multi-objective optimization design and control of plug-in hybrid electric vehicle powertrain for minimization of energy consumption, exhaust emissions and battery degradation. Energy Conversion and Management, 234, (2021) 113909. https://doi.org/10.1016/j.enconman.2021.113909

[12] A. Nasri, B. Gasbaoui, Neuro-Fuzzy control for four Wheels electric vehicle safety. Journal of Renewable Energies, 20(1), (2017) 91–98. https://doi.org/10.54966/jreen.v20i1.612

[13] J.G. Niu, F.L. Pei, S. Zhou, T. Zhang, Multi-Objective Optimization Study of Energy Management Strategy for Extended-Range Electric Vehicle. Advanced Materials Research, 694–697, (2013) 2704–2709. https://doi.org/10.4028/www.scientific.net/AMR.694-697.2704

[14] H. Bederina, M. Hifi, A hybrid multi-objective evolutionary optimization approach for the robust vehicle routing problem. Applied Soft Computing, 71, (2018) 980–993. https://doi.org/10.1016/j.asoc.2018.07.014

[15] X. Duan, F. Schockenhoff, A. Koch, Implementation of Driving Cycles Based on Driving Style Characteristics of Autonomous Vehicles. World Electric Vehicle Journal, 13(6), (2022) 108. https://doi.org/10.3390/wevj13060108

[16] K. Djermouni, A. Berboucha, K. Ghedamsi, D. Aouzellag, S. Tamalouzt, Energy Management Applied To Non-Autonomous Photovoltaic Station For Hybrid Vehicle Loading. Journal of Renewable Energies, 1(1), (2024) 33 – 45. https://doi.org/10.54966/jreen.v1i1.1172

[17] J. Guo, H. He, C. Jia, S. Guo, The Energy Management Strategies for Fuel Cell Electric Vehicles: An Overview and Future Directions. World Electric Vehicle Journal, 16(9), (2025) 542. https://doi.org/10.3390/wevj16090542

[18] X. Yang, Y. Wang, Genetic Algorithm-Based Energy Management Strategy for Fuel Cell Hybrid Electric Vehicles. World Electric Vehicle Journal, 16(8), (2025) 467. https://doi.org/10.3390/wevj16080467

[19] S. Zhou, Z. Wen, X. Zhi, J. Jin, Sh. Zhou, (2019) Genetic Algorithm-Based Parameter Optimization of Energy Management Strategy and Its Analysis for Fuel Cell Hybrid Electric Vehicles. SAE Technical Paper. https://doi.org/10.4271/2019-01-0358

[20] F. Tazerart, Z. Mokrani, D. Rekioua, T. Rekioua, Direct torque control implementation with losses minimization of induction motor for electric vehicle applications with high operating life of the battery. International Journal of Hydrogen Energy, 40(39), (2015) 13827–13838. https://doi.org/10.1016/j.ijhydene.2015.04.052

[21] X. Hu, S. Liu, K. Song, Y. Gao, T. Zhang, Novel Fuzzy Control Energy Management Strategy for Fuel Cell Hybrid Electric Vehicles Considering State of Health. Energies, 14(20), (2021) 6481. https://doi.org/10.3390/en14206481

[22] A. Mazouzi, N. Hadroug, W. Alayed, A. Hafaifa, A. Iratni, A. Kouzou, Comprehensive optimization of fuzzy logic-based energy management system for fuel-cell hybrid electric vehicle using genetic algorithm. International Journal of Hydrogen Energy, 81, (2024) 889–905. https://doi.org/10.1016/j.ijhydene.2024.07.237

[23] Ballard Power Systems, (2017) Fuel cell catalyst materials, non-precious metal catalyst. Technical Note, Canada. https://www.ballard.com/wp-content/uploads/2024/10/fuel-cell-catalyst-materials.pdf

[24] V. Balaji, P. Jeevanantham, M. M. Krishnan, Analysis of Flow Parameters in Fuel Cell for Efficient Power Generation. International Journal of Engineering and Innovative Technology, 2(9), (2013) 160-164.

[25] I.S. Martin, A. Ursúa, P. Sanchis, Modelling of PEM Fuel Cell Performance: Steady-State and Dynamic Experimental Validation. Energies, 7(2), (2014) 670-700. https://doi.org/10.3390/en7020670

[26] R.W. Erickson, D. Maksimović, (2001). Fundamentals of Power Electronics (2nd ed). Springer, New York. https://doi.org/10.1007/b100747

[27] J.T. Pukrushpan, A.G. Stefanopoulou, H. Peng, (2004). Control of Fuel Cell Power Systems. Springer, London. https://doi.org/10.1007/978-1-4471-3792-4

[28] D.G. Holmes, T.A. Lipo, (2003). Pulse Width Modulation for Power Converters: Principles and Practice. IEEE Press. https://doi.org/10.1109/9780470546284

[29] M. Ehsani, Y. Gao, S. Longo, K. Ebrahimi, (2018) Modern Electric, Hybrid Electric, and Fuel Cell Vehicles (3rd ed.). CRC Press. https://doi.org/10.1201/9781420054002

[30] R. Krishnan, (2010). Permanent Magnet Synchronous and Brushless DC Motor Drives. CRC Press.

[31] L.A. Dicks, D.A.J. Rand, (2018) Fuel Cell Systems Explained. John Wiley & Sons Ltd, New York. https://doi.org/10.1002/9781118706992

[32] M. Rahimi- Esbo, A.A. Ranjbar, S.M. Rahgoshay, Analysis of water management in PEM fuel cell stack at dead-end mode using direct visualization. Renewable Energy, 162, (2020) 212–221. https://doi.org/10.1016/j.renene.2020.06.078

[33] J. Zhou, J. Liu, Q. Su, C. Feng, X. Wang, D. Hu, F. Yi, C. Jia, Z. Fan, S. Jiang, Heat Dissipation Enhancement Structure Design of Two-Stage Electric Air Compressor for Fuel Cell Vehicles Considering Efficiency Improvement. Sustainability, 14(12), (2022) 7259. https://doi.org/10.3390/su14127259

[34] S.F. Tie, C. W. Tan, A review of energy sources and energy management system in electric vehicles," Renewable and Sustainable Energy Reviews, 20, (2013), 82–102. https://doi.org/10.1016/j.rser.2012.11.077

[35] S. Onori, L. Serrao, G. Rizzoni, (2016). Introduction. In: Hybrid Electric Vehicles. SpringerBriefs in Electrical and Computer Engineering. Springer, London. https://doi.org/10.1007/978-1-4471-6781-5_1

Acknowledgements

The authors are grateful for the moral support they received from the Laboratory of Management, Maintenance, and Rehabilitation of Facilities and Urban Infrastructure of Souk Ahras. We also want to express our gratitude to those in charge of this scholarly journal.

Authors Contribution Statement

Bilal Soltani: Conceptualization, Methodology, Software, Formal analysis, Investigation, Data curation, Writing – Original Draft, Visualization. Nedjem-Eddine Benchouia: Supervision, Validation, Writing – Review & Editing, Project administration. Abdelghani Guechi: Investigation, Resources, Writing – Review & Editing.
All the authors have read and agreed to the published version of the manuscript.

Funding

The authors declare that no funds, grants or any other support were received during the preparation of this manuscript.

Conflict of Interest

The authors affirm that there are no conflicts of interest in connection with the publication of this article. All authors have no known competing financial interest or personal relationships that could have reasonably influenced the work reported in this article.

Competing Interests

The authors declare that there are no conflicts of interest regarding the publication of this manuscript.

Data Availability

The data supporting the findings of this study can be obtained from the corresponding author upon reasonable request.

Has this article screened for similarity?

Yes

About the License